
Fast Abductive Learning by Similarity-based Consistency Optimization

Yu-Xuan Huang¹, Wang-Zhou Dai², Le-Wen Cai¹, Stephen Muggleton², Yuan Jiang¹

¹National Key Laboratory for Novel Software Technology

Nanjing University, Nanjing 210023, China

{huangyx, cailw, jiangy}@lamda.nju.edu.cn

²Department of Computing, Imperial College London, London SW7 2AZ, UK

{w.dai, s.muggleton}@imperial.ac.uk

Abstract

To utilize the raw inputs and symbolic knowledge simultaneously, some recent neuro-symbolic learning methods use abduction, i.e., abductive reasoning, to integrate sub-symbolic perception and logical inference. While the perception model, e.g., a neural network, outputs some facts that are inconsistent with the symbolic background knowledge base, abduction can help revise the incorrect perceived facts by minimizing the inconsistency between them and the background knowledge. However, to enable effective abduction, previous approaches need an initialized perception model that discriminates the input raw instances. This limits the application of these methods, as the discrimination ability is usually acquired from a thorough pre-training when the raw inputs are difficult to classify. In this paper, we propose a novel abduction strategy, which leverages the similarity between samples, rather than the output information by the perceptual neural network, to guide the search in abduction. Based on this principle, we further present ABductive Learning with Similarity (ABLSim) and apply it to some difficult neuro-symbolic learning tasks. Experiments show that the efficiency of ABLSim is significantly higher than the state-of-the-art neuro-symbolic methods, allowing it to achieve better performance with less labeled data and weaker domain knowledge.

1 Introduction

To address the limitations of current machine learning methods, the next generation of Artificial Intelligence calls for the integration of data-driven machine learning and knowledge-driven reasoning such as logic inference [1]. Neuro-Symbolic Learning [8, 22] and Statistical Relational AI [23] are representative works in this direction. However, most of these approaches try to approximate logical calculus with differentiable functions using distributed representations in a neural network, and train the model in an end-to-end manner, which usually demand a large number of labeled data.

Abductive Learning (ABL) [5, 29] is a novel framework attaching machine learning models to a first-order logical reasoning model while preserving the full expressive power of each side: The machine learning model learns to convert raw input data (e.g., images, text) into symbolic representations, and the logical model tries to reason about them. Because ABL allows full-featured logical reasoning, it can directly consult symbolic background knowledge bases and reduce the requirement for massive labeled data. The logical reasoning model adopts *abductive reasoning* [20], or *abduction*, to search for the labels of the unlabeled instances, which are used for updating the machine learning model. Because abductive reasoning is non-deterministic, for each unlabeled instance there could be multiple *abduced labels*. To choose the best labels, one needs to *minimize the inconsistency* between the abduced labels and the symbolic background knowledge.

Hence, a well-designed consistency measure improves the quality of the abduced labels and leads to a high-performance model. For example, some approaches take the consistency score as the size of the largest subset of unlabeled examples with abduced labels that are consistent with knowledge base, leading to a subset-selection problem that is difficult to solve [5, 29]; some other works measure the confidence of the predicted labels by the perceptual machine learning model, which could be unreliable when the model is under-trained [19, 4, 2].

According to its definition, *abduction* refers to the process of inferring specific facts that give the best explanation to observations based on background knowledge [20]. Hence, not only the symbolized information—the labels predicted by perception model and the symbolic background knowledge base, but also the observed raw representation of the inputs contribute to the goodness of abduced labels. For example, when babies start learning an unknown language, although they could not make sense of the acoustic syllables in a sentence, they can amazingly learn from a handful of examples and understand a few words by distinguishing different sound patterns (raw representation) as well as identifying frequently occurred syllable combinations (symbolic relations) [9].

Inspired by this phenomenon, we develop a similarity-based consistency measure for abduction, which takes the idea that samples in the same category are similar in feature space while samples of different classes are dissimilar. It can be regarded as the clustering initialization for the perception model [29], and then the metric for clustering in embedding space is improved when the model gets updated by the abduced labels during training. Applying this principle, we propose ABductive Learning with Similarity (ABLSim), which adopts beam search to solve the optimization problem of finding the best abduced labels. We verify the effectiveness of ABLSim on four neuro-symbolic tasks. Compared with other methods, ABLSim can abduce higher quality labels for unlabeled data and accelerate the model training, bringing a significantly better performance. Moreover, even when we increase the difficulty of abduction by removing some rules from the knowledge base, ABLSim still achieves comparable results as the other abduction-based neuro-symbolic learning methods with a full knowledge base.

2 Related Work

Neuro-symbolic (NeSy) learning [8, 22] proposes to enhance machine learning with symbolic reasoning. It tries to learn the ability for both perception from the environment and reasoning from what has been perceived. Most of the approaches model this pipeline with an end-to-end deep neural network, in which a symbolic domain knowledge base is used for building the structure of neural networks [8, 25, 11, 10, 24, 27]. However, most of these methods replace the symbolic representation with distributed representation and approximate logic inference with fuzzy operations. As a consequence, they usually require a large amount of labeled training data and are difficult to extrapolate.

Probabilistic Logic Program (PLP) [6] and Statistical Relational Learning (SRL) [15, 23] supply symbolic models with a probabilistic semantic and preserve the logical formulation. PLP extends first-order logic to accommodate probabilistic groundings to include probabilistic inference; SRL tries to leverage domain knowledge to construct a probabilistic graphical model structure for statistical inference. They usually require direct semantic level input and are difficult to be applied to raw input data such as images. A typical exception in this area is DeepProbLog [21], which unifies probabilistic logical inference with neural network training by gradient descent. However, due to the exponential complexity of the probabilistic distribution on the Herbrand base, the probabilistic inference in these methods could be inefficient for complicated tasks.

Recently, some approaches leverage abduction to train machine learning and perform logical reasoning simultaneously, e.g., the Abductive Learning (ABL) [5, 29] framework. ABL uses machine learning models to predict pseudo-labels for the unlabeled data, and then uses first-order logical abduction to revise them and update the machine learning model. The abduction searches for a set of revised pseudo-labels to minimize the inconsistency between data and knowledge base. However, when the model is under-trained, the revision becomes difficult because the predicted pseudo-labels are mostly incorrect, and the abduction could be easily trapped in local optima [4, 2]. The Neural-Grammar-Symbolic model (NGS) [19] shares a similar idea of abduction. It takes context-free grammar as the knowledge base and uses Markov Chain Monte Carlo (MCMC) sampling to revise the pseudo-labels according to their posterior, which suffers from the same problem when the neural

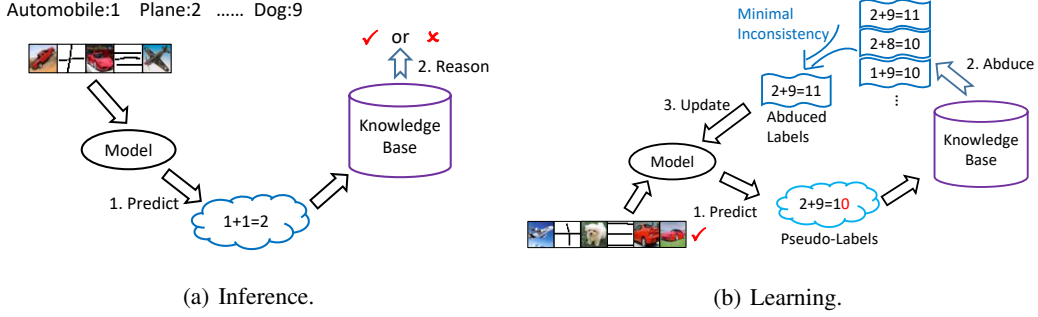


Figure 1: An example of the inference and learning process of ABL. In the inference process, the input data is a decimal equation represented by several CIFAR-10 images, e.g., the images “plane” represent digit 1, “automobile” for digit 2, “dog” for digit 9. The final output is the reasoning result on both symbols predicted by the perception model and the knowledge base. In the learning stage, the reasoning model abduces several consistent revised pseudo-labels and searches for the best one by minimizing the inconsistency, which are then used to update the perception model.

network is under-trained. Different from these approaches, ABLSim considers the similarity between input examples in the feature space rather than the output space.

3 Abductive Learning

3.1 Inference

The Abductive Learning (ABL) framework contains a perception model and a reasoning model. The perception model is used for mapping the raw input data $\mathbf{x} \in \mathcal{X}$ into discrete symbols $z \subseteq \mathcal{Z}$, where \mathcal{X} is the input space and \mathcal{Z} is the output space of the perception model; \mathbf{x} and z are the input *example* and extracted symbols, respectively, where $\mathbf{x} = \{x_1, x_2, \dots\}$ and $z = \{z_1, z_2, \dots\}$ are the bags of meaningful *instances* detected from \mathbf{x} and the corresponding symbolic labels. For the example in Figure 1, an input image of the equation is \mathbf{x} ; the segmented instances of CIFAR-10 images and operation symbols are x_i ; the sequence of predicted equation string is z , with each of its characters as z_i ; whether the equation satisfies KB is denoted as $y = True$ or $y = False$.

The reasoning model contains knowledge base KB of first-order logic rules, which receives the symbols z and reasons about the final output $y \in \mathcal{Y}$. Note that \mathcal{Z} and \mathcal{Y} are subsets of the Herbrand base of KB , i.e., elements in $\mathcal{Z} \cup \mathcal{Y}$ are ground facts of the predicates defined in KB . For example, given the symbolic rules of decimal arithmetic, the reasoning model would output a ground fact $y = True$ when the input fact is $z = “1+1=2”$, and a ground fact $y = False$ when input is $z = “1+9=10”$. Figure 1(a) gives an example of the inference process in the *CIFAR-10 Decimal Equation Decipherment* task (cf. Section 6.3).

3.2 Abductive Reasoning

Abduction (i.e. *abductive reasoning*) [14, 20] is a basic form of logical inference that seeks the best explanation for observations based on implication. It is a non-deterministic process that may have multiple answers. For example, when observing an arithmetic puzzle “*dog + cat = 2*”, based on our background knowledge in mathematics, we could explain it with three abduced facts: “*dog = cat = 1*”, “*dog = 2 ∧ cat = 0*” or “*dog = 0 ∧ cat = 2*”.

3.3 Learning

Formally, given unlabeled data $\mathbf{X} = \{\mathbf{x}^{(1)}, \mathbf{x}^{(2)}, \dots\}$, the knowledge base KB and the final desired output $Y = \{y^{(1)}, y^{(2)}, \dots\}$, the target is to learn a perception model $f : \mathcal{X} \mapsto \mathcal{Z}$ that accurately predicts the labels of the input instances that together with KB entails y . Since we do not have any supervision on z , we call it *pseudo-label* just like in *weakly-supervised learning* [28].

The ABL framework involves three steps—predict pseudo-labels, abduce revised labels and update the model. First, the perception model f is used to obtain the symbolic predictions $z = f(x)$ as pseudo-labels. Then ABL revises the pseudo-labels z to \bar{z} by abductive reasoning. Usually, there are several candidates \bar{z} that are consistent with KB . The reasoning model abduces the most likely correct pseudo-labels \bar{z} under the principle of *minimal inconsistency* between the data and knowledge base. Finally, ABL treats the \bar{z} as ground-truth labels to update the perception model, and the above routine repeats iteratively.

Figure 1(b) gives an example, where the ground-truth labels of the input are “2+9=11” and $y = True$. The perception model f predicts the wrong pseudo-labels $z = \text{“2+9=10”}$. After minimizing the inconsistency in abduction, $\bar{z} = \text{“2+9=11”}$ is selected as the final revised label to update f .

3.4 Consistency Measure

Consistency measure for abduction plays an important role in ABL. It is used to guide the search of the abduced labels \bar{z} from the set of consistent candidate labels $\mathbb{A} = \{\bar{z} \mid KB \cup \bar{z} \models y\}$, where \models means logical entailment. Because \bar{z} will be treated as ground-truth to update the perception model, whether and how the model improves mainly depends on the design of this consistency measure. Current consistency measures mainly depend on the model’s output labels or confidence, which could perform poorly when f is inaccurate or not properly initialized [4, 2]. We verify this in our experiments in Section 6.

4 The Similarity-based Consistency Measure

We propose a similarity-based consistency measure for abduction, which takes the idea that samples in the same category are similar in feature space while samples of different classes are dissimilar. It is motivated by how humans perform abductive reasoning. Take the example in Figure 1(b). If we misclassified the last image to digit 0 and the prediction becomes “2+9=10”, which is inconsistent with the knowledge base. Revisions “1+9=10”, “2+8=10” and “2+9=11” are all consistent revisions. By looking at the images directly, we could observe that the last two images are similar, while the other pairwise combinations of these images look quite different. Therefore, the last two images probably share the same label. Finally, we conclude that “2+9=11” are the most likely correct labels, which could be regarded as the best abduced labels.

Given the final output y and knowledge base KB , let \mathbb{A} be the set of all consistent candidates by abductive reasoning, i.e., $\mathbb{A} = \{\bar{z} \mid KB \cup \bar{z} \models y\}$. The consistency optimization problem is equivalent to selecting the best revised labels \bar{z} in \mathbb{A} , which can be formalized as follows:

$$\max_{\bar{z} \in \mathbb{A}} \text{SimilarityScore}(\mathbf{x}, \bar{z}), \quad (1)$$

where the SimilarityScore measures the consistency of the revised labels \bar{z} . We define the consistency as the average difference between each sample’s inter-class distance and intra-class distance:

$$\text{SimilarityScore}(\mathbf{x}, \bar{z}) = \frac{1}{|\mathbf{x}|} \sum_{x_i \in \mathbf{x}} (\text{InterclassDis}(x_i, \bar{z}) - \text{IntraclassDis}(x_i, \bar{z})). \quad (2)$$

The inter-class distance $\text{InterclassDis}(x_i, \bar{z})$ of sample x_i stands for the average distance of other instances x_j that have different revised labels as x_i ; while the intra-class distance $\text{IntraclassDis}(x_i, \bar{z})$ defines the average distance of other instances x_j that have the same revised labels as x_i , i.e.,

$$\text{InterclassDis}(x_i, \bar{z}) = \frac{1}{|\mathbb{D}_{i,\bar{z}}|} \sum_{x_j \in \mathbb{D}_{i,\bar{z}}} \text{Dis}(x_i, x_j), \quad (3)$$

$$\text{IntraclassDis}(x_i, \bar{z}) = \frac{1}{|\mathbb{S}_{i,\bar{z}}|} \sum_{x_j \in \mathbb{S}_{i,\bar{z}}} \text{Dis}(x_i, x_j), \quad (4)$$

where $\mathbb{D}_{i,\bar{z}} = \{x_j \mid \bar{z}_j \neq \bar{z}_i, j \neq i\}$ is the set of instances whose labels are *different* from x_i ’s, and $\mathbb{S}_{i,\bar{z}} = \{x_j \mid \bar{z}_j = \bar{z}_i, j \neq i\}$ is the set of the other instances that share the *same* revised labels as x_i . Note that $\mathbb{D}_{i,\bar{z}} \cup \mathbb{S}_{i,\bar{z}} \cup x_i = \mathbf{x}$. $\text{Dis}(x_i, x_j)$ is the distance between x_i and x_j , which will be explained later. If $|\mathbb{D}_{i,\bar{z}}| = 0$ or $|\mathbb{S}_{i,\bar{z}}| = 0$, where the denominator becomes 0, we use the

Algorithm 1 ABLSim Learning

Input: Unlabeled data $\mathbf{X} = (\mathbf{x}^{(1)}, \mathbf{x}^{(2)}, \dots, \mathbf{x}^{(m)})$; Final output $y = (y^{(1)}, y^{(2)}, \dots, y^{(m)})$;
Current model f ; Knowledge base KB ; Beam width (beam size of beam search) b

Output: Model f

- 1: **for** $t = 1$ **to** T **do**
- 2: $\mathbb{A} \leftarrow \emptyset$ # the candidate labels
- 3: **for** $k = 1$ **to** m **do**
- 4: $\mathbf{z}^{(k)} \leftarrow f(\mathbf{x}^{(k)})$ # generate pseudo-labels
- 5: $\mathbb{A}^{(k)} \leftarrow \text{Abduce}(KB, \mathbf{z}^{(k)}, y^{(k)})$ # abduce all consistent revised pseudo-labels
- 6: $\mathbb{A} \leftarrow \mathbb{A} \times \mathbb{A}^{(k)}$ # Cartesian product
- 7: $\mathbf{x} \leftarrow \mathbf{X}[1 : k]$
- 8: $\text{score} \leftarrow \emptyset$ # the score of each candidate labels
- 9: **for** $\bar{\mathbf{z}} \in \mathbb{A}$ **do**
- 10: $\text{score.append}(\text{Score}(\mathbf{x}, \bar{\mathbf{z}}))$ # get the score of candidate labels according to Eq. (12)
- 11: **end for**
- 12: $\mathbb{A} \leftarrow \text{TopN}(\mathbb{A}, \text{score}, b)$ # select 'b' candidate labels in \mathbb{A} with the highest score
- 13: **end for**
- 14: $\bar{\mathbf{Z}} \leftarrow \text{TopN}(\mathbb{A}, \text{score}, 1)$ # select the label in \mathbb{A} with the highest score
- 15: $f \leftarrow \text{Update}(f, \mathbf{X}, \bar{\mathbf{Z}})$ # update model f using data \mathbf{X} and abduced labels $\bar{\mathbf{Z}}$
- 16: **end for**

average inter-class/intra-class distance of other x_j as the estimated distance of x_i . The details on the calculation when the denominator becomes 0 are shown in the supplementary material.

Combining (1)-(4), the similarity-based consistency measure optimization problem becomes:

$$\max_{\bar{\mathbf{z}} \in \mathbb{A}} \frac{1}{|\mathbf{x}|} \sum_{x_i \in \mathbf{x}} \left(\frac{1}{|\mathbb{D}_{i, \bar{\mathbf{z}}}|} \sum_{x_j \in \mathbb{D}_{i, \bar{\mathbf{z}}}} \text{Dis}(x_i, x_j) - \frac{1}{|\mathbb{S}_{i, \bar{\mathbf{z}}}|} \sum_{x_j \in \mathbb{S}_{i, \bar{\mathbf{z}}}} \text{Dis}(x_i, x_j) \right). \quad (5)$$

The distance $\text{Dis}(x_i, x_j)$ in (3)-(5) measures the similarity between instances x_i and x_j , where the higher the similarity, the smaller the distance. It can be represented as follows:

$$\text{Dis}(x_i, x_j) = \text{Distance}(\phi(x_i), \phi(x_j)). \quad (6)$$

where ϕ is the feature map function. For example, for images or text, we can use a neural network as ϕ to extract the embedding for samples; for tabular data, ϕ can be the normalization function. In practice, we can use any appropriate metrics in (6). In this work, we use the cosine distance in our implementation, i.e., $\text{Dis}(x_i, x_j) = \text{CosineDistance}(\phi(x_i), \phi(x_j))$.

Obviously, maximizing the score in (2) means maximizing the average gap between $\text{InterclassDis}(x_i, \bar{\mathbf{z}})$ and $\text{IntraclassDis}(x_i, \bar{\mathbf{z}})$. In other words, among all revised labels candidates that are consistent, the one with a large inter-class distance and a small intra-class distance is preferred.

Calculating the similarity between instances does not depend on any supervised training. Hence, one could use any unsupervised learning approaches to obtain a good ϕ without accessing any label information [3, 7]. This consistency measure can be regarded as an implicit clustering initialization on the output space of function ϕ [29]. In addition, if we use the perception model f 's embedding layer as the function ϕ , the ϕ and the distance measurement could be further improved during the subsequent neuro-symbolic learning and accelerates the abduction reasoning.

5 Abductive Learning with Similarity

Based on the proposed consistency measure, we present the Abductive Learning with Similarity (ABLSim) approach, which is optimized through a greedy beam search. And then we show that ABLSim can be simply combined with other consistency measures to enhance abduction-based neuro-symbolic learning. Algorithm 1 shows an outline of ABLSim.

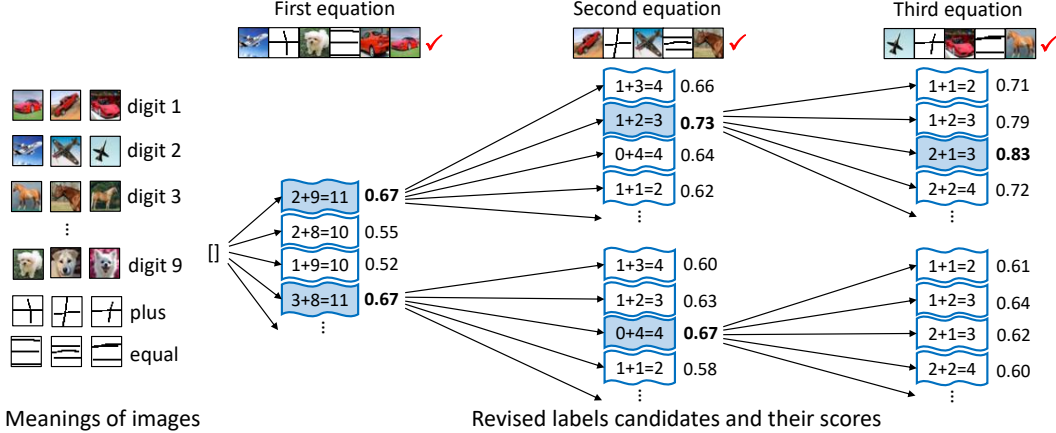


Figure 2: An example of beam search in ABLSim. It involves three unlabeled and consistent equations whose ground-truth labels are “2+9=11”, “1+2=3”, “2+1=3”, and the beam width is 2. In the first iteration, after computing the scores, “2+9=11” and “3+8=11” are kept in the candidate set. In the second iteration, “2+9=11 1+2=3” and “3+8=11 0+4=4” rank top 2 among all candidate revised labels, while other candidates are pruned. In the last iteration, we get the final abduced label “2+9=11 1+2=3 2+1=3” according to the computed scores of consistency measure.

5.1 Optimization

One possible situation when applying ABLSim is that the number of instances in \mathbf{x} is usually small, and for some example $\mathbf{x}^{(k)}$ there is no $\langle i, j \rangle$ such that $\bar{z}_i^{(k)} = \bar{z}_j^{(k)}$, making it challenging to calculate the intra-class distance. For example in Figure 1(b), the size $|\mathbf{x}| = 6$, and for the revised pseudo-labels candidate $\bar{z} = \text{“2+9=11”}$, we could not measure the intra-class distance of the first image x_1 because there is no other sample x_j whose revised label \bar{z}_j is digit 2. Moreover, even if instances with the same revised label exist, the average distance may deviate due to limited samples.

To get a sound and reliable score for consistency measure, we borrow some more samples to conduct the abductive reasoning. Assume that there are m examples, denoted as $\mathbf{x}^{(1)}, \mathbf{x}^{(2)}, \dots, \mathbf{x}^{(m)}$. Each example $\mathbf{x}^{(k)}$ has a corresponding final output $y^{(k)}$ and the candidate set of revised labels is $\mathbb{A}^{(k)}$. If labeled data exists, it can also be regarded as bags of instances, whose candidate pseudo-label set $\mathbb{A}^{(k)}$ contains only the ground-truth labels. Let $\mathbf{X} = (\mathbf{x}^{(1)}, \mathbf{x}^{(2)}, \dots, \mathbf{x}^{(m)})$ be the set of input examples, and $\bar{\mathbf{Z}} = (\bar{z}^{(1)}, \bar{z}^{(2)}, \dots, \bar{z}^{(m)})$ be the set of corresponding bags of abduced labels. If $\bar{\mathbf{Z}}$ is consistent with knowledge base, it should be an element of the Cartesian product of $\mathbb{A}^{(k)}$, i.e., $\bar{\mathbf{Z}} \in \mathbb{A}^{(1)} \times \mathbb{A}^{(2)} \times \dots \times \mathbb{A}^{(m)}$. The abduction problem for set \mathbf{X} can be formalized as follows:

$$\max_{\bar{\mathbf{Z}}} \text{Score}(\mathbf{X}, \bar{\mathbf{Z}}), \quad (7)$$

$$s.t. \quad \mathbf{X} = (\mathbf{x}^{(1)}, \mathbf{x}^{(2)}, \dots, \mathbf{x}^{(m)}), \quad (8)$$

$$\bar{\mathbf{Z}} \in \mathbb{A}^{(1)} \times \mathbb{A}^{(2)} \times \dots \times \mathbb{A}^{(m)}, \quad (9)$$

$$\mathbb{A}^{(k)} = \{\bar{z} \mid KB \cup \bar{z} \models y^{(k)}\}. \quad (10)$$

This is a combinatorial optimization problem where the search space of $\bar{\mathbf{Z}}$ grows exponentially with m . ABLSim uses beam search to solve this optimization problem greedily. Eventually, the element with the highest score in the final candidate set \mathbb{A} will be selected as the best abduced labels.

Figure 2 gives an example of the beam search in ABLSim in the *CIFAR-10 Equation Decipherment* task. There are three unlabeled examples $\mathbf{x}^{(1)}, \mathbf{x}^{(2)}, \mathbf{x}^{(3)}$ consistent with the knowledge base and the beam width $b = 2$. In each iteration, ABLSim keeps the top-2 candidates ranked by their scores. The final abduced label is $\bar{\mathbf{Z}} = \text{“2+9=11 1+2=3 2+1=3”}$, which is the ground-truth label.

The above ABLSim algorithm could be accelerated by GPU and parallel computations. The basic idea is that the score of each candidate label \bar{z} in \mathbb{A} (cf. Line 9-10 in Algorithm 1) can be computed separately, and we formulate the calculation as matrix operations for parallel computations with GPU.

Table 1: Image test accuracy and convergence time of different methods. The convergence time stands for the time taken to accuracy 95% in handwritten images and 85% for CIFAR-10. NGS-dft stands for NGS with default parameters, and NGS-opt for the fine-tuned optimal parameters. We set the time limit to 10 hours for all tasks. • indicates ABLSim is significantly better than compared methods (paired t-tests at 95% significance level)

	Method	Addition	Addition (CIFAR)	HWF	HWF (CIFAR)
Acc / %	DeepProbLog	96.5±0.5•	21.6±1.7•	32.2±0.6•	15.2±2.6•
	NGS-dft	39.9±54.1•	38.7±35.1•	99.6±0.2•	23.8±6.3•
	NGS-opt	98.5±0.3•	88.7±0.8	99.6±0.2•	66.0±14.5•
	ABLSim (ours)	98.8±0.1	88.9±0.5	99.9±0.1	88.4±0.7
Time / s	DeepProbLog	396±3	time out	time out	time out
	NGS-dft	time out	time out	299±36	time out
	NGS-opt	46±4	6954±558	240±7	time out
	ABLSim (ours)	42±5	6066±79	130±4	7263±122

During the beam search, the score of each \bar{z} is updated incrementally based on the previous results, which further reduces the memory and time consumption. Please refer to the supplementary material for details.

5.2 Combining Similarity and Confidence in Consistency Measure

ABLSim can also be combined with other consistency measures. For example, the confidence score of a revised pseudo-label \bar{z} could be defined as follows:

$$\text{ConfidenceScore}(\mathbf{x}, \bar{z}) = \frac{1}{|\mathbf{x}|} \prod_{x_i \in \mathbf{x}} \text{Confidence}(x_i, \bar{z}_i), \quad (11)$$

where $\text{Confidence}(x_i, \bar{z}_i)$ indicates the confidence that sample x_i belongs to label \bar{z}_i .

Combining (2) and (11), we get the final score for ABLSim’s consistency measure:

$$\text{Score}(\mathbf{x}, \bar{z}) = \theta \cdot \text{SimilarityScore}(\mathbf{x}, \bar{z}) + (1 - \theta) \cdot \text{ConfidenceScore}(\mathbf{x}, \bar{z}), \quad (12)$$

where $\theta \in \mathbb{R}$ is the weighting coefficient. The similarity score and confidence score need to be normalized before computing the final score.

6 Experiments

This section presents the experimental results on four neuro-symbolic tasks, including two benchmark datasets and two hard tasks with increased perception difficulty, to demonstrate that ABLSim can perform more efficient and effective abduction than previous state-of-the-art methods by leveraging the similarity among samples. Furthermore, we verify whether it can help the perception model learn faster and achieve better performance with less labeled data and weaker domain knowledge. All experiments are repeated five times on a server with Intel Xeon Gold 6248R CPU and Nvidia Tesla V100S GPU. In experiments, we simply fix the coefficient θ of ABLSim to 0.96, though it may be better to let it vary with training. The hyperparameters of ABLSim are determined by cross-validation on training data. The code is available for download¹.

6.1 MNIST (CIFAR-10) Addition

This task was first introduced in [21], the inputs are pairs of MNIST [17] images and the outputs are their sums. We also prepare a hard version of this task by replacing the MNIST images with CIFAR-10 [16] images. We compare ABLSim with the Neural-Grammar-Symbolic (NGS) model [19] (with default and fine-tuned parameters) and DeepProbLog [21]. All methods share the same knowledge base and perception model (LeNet [17] for MNIST and ResNet-50 [12] for CIFAR-10), which are initialized randomly. The feature for calculating the similarity score is obtained from the second last layer in the perceptual neural net.

Table 1 shows the experimental results. In the MNIST Addition task, all methods except NGS-dft converge. DeepProbLog converges slowly because computing gradients of the probabilistic logic

¹<https://github.com/AbductiveLearning/ABLSim>

program is time-consuming. The performance of NGS-dft is greatly affected by initialization, which leads to a large standard deviation in the table. For the CIFAR-10 version, DeepProbLog and NGS-dft fail to converge, while NGS-opt converges slower than ABLSim, which solves all tasks efficiently and achieves higher accuracy.

6.2 Handwritten Formula Recognition

The HWF dataset [19] contains images of decimal formulas and their computed results. We also create a (perceptual) harder version by replacing the digit images with CIFAR-10 [16] images.

The perception neural networks are initialized randomly for all methods. Note that the HWF in the original paper of NGS includes length-one equations as a pre-training curriculum, which are deleted in our experiments. Thus our results are different from those in [19].

As shown in Table 1, ABLSim significantly outperforms others by time efficiency and predictive accuracy. Because the background knowledge is the same, this result verifies the benefit of leveraging the similarity-based consistency optimization. Both NGS and DeepProbLog are trapped in local minimum and fail to converge in the hard version tasks, this is probably caused by the unreliable confidence output from the perception neural network when it is not pre-trained.

6.3 CIFAR-10 Decimal Equation Decipherment

6.3.1 Dataset and Knowledge base

This task is the most challenging one in our experiments, which extends the Digital Binary Additive equations experiment in ABL [5] with *decimal* digits. The input contains images of an arithmetic equation and the output is the label of its correctness. Instead of learning binary equations represented by MNIST images, here we use CIFAR-10 [16] images to encode decimal equations. An example of this dataset is shown in Figure 2. The task’s inputs are sequential images of randomly generated decimal equations, which consist of twelve symbols (0,1,⋯,9,+,,=). Besides, the knowledge base contains symbolic rules about how to carry out decimal addition operations. The correctness labels (*True* or *False*) of training equations are provided in the form of logical facts.

6.3.2 Experimental Setup

We compare ABLSim with four baselines: 1) **ABL**: Abductive learning [5] that maximizes consistency with minimal revisions. If multiple abduced labels have the minimal revisions, it would randomly select one. 2) **ABL-Conf**: Abductive learning that measures consistency using only the confidence predicted by neural net, i.e., $\theta = 0$ in equation (12). 3) **ABL-pre-train**: ABL with model pre-trained on a small set of labeled images. 4) **ABL-Conf-pre-train**: ABL-Conf with a pre-trained network. ABLSim uses the perception model’s embedding layer to calculate the similarity. For the non-pre-trained methods, including ABLSim, the perception model, a ResNet-50 [12], is initialized by self-supervised learning [3] on training images. Note that this process is unsupervised and does NOT use any image labels.

6.3.3 Results

Learning Curve. The learning curves of all models are shown in Figure 3(a). The proposed ABLSim converges much faster and achieves higher accuracy than other methods. ABL-Conf and ABL fail to converge and get low accuracy because their abduction processes are based on the pseudo-labels or label confidence predicted by the perception model, which are unreliable when there lacks supervised pre-train. Both ABL and ABL-pre-train are inferior to their ‘-Conf’ versions, indicating that pseudo-label confidence is helpful. Starting from high initial accuracy, ABL-Conf-pre-train gets a similar accuracy as ABLSim, but it converges slower than our presented ABLSim, which learns without any supervised pre-training and has the fastest converge rate.

Rate of Successful Abduction. Figure 3(b) illustrates the curves of different methods’ abduction success rate, i.e., the proportion of the correctly abduced labels. ABLSim converges faster and achieves a nearly optimal result, where the abduced labels are exactly the ground-truth labels. In the first few iterations, the abduction success rate is relatively low. However, the extracted embeddings of

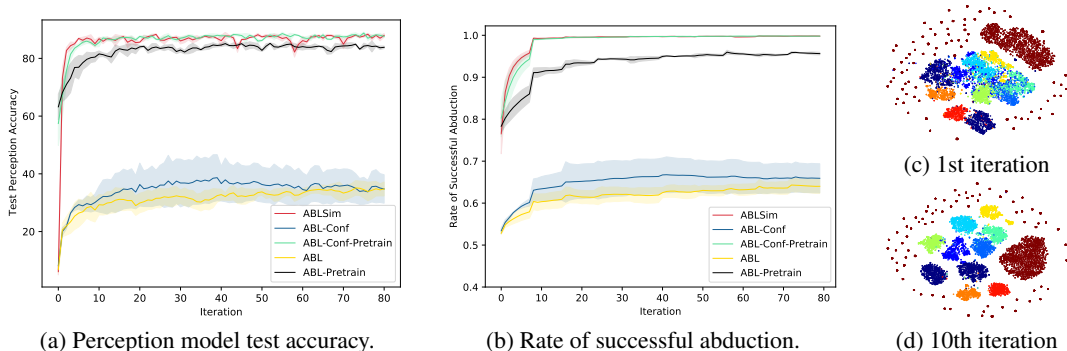


Figure 3: Learning curves (a & b) and the t-SNE visualization of the learned embeddings (c & d).

Table 2: The rate of successful abduction w.r.t. different beam width in the first iteration.

Beam Width	16	32	64	128	256	512	1024	2048
Successful Abductions	62%	63%	65%	71%	72%	73%	75%	75%

images are gradually improved during training, which provide a better similarity metric for abductive reasoning. Therefore, the rate of successful abduction reaches 1.0 just in a few iterations.

Embedding Visualization. To verify whether the extracted embeddings of neural network are improved during training, we plot t-SNE [26] visualizations on the second last layer of neural network that we use for calculating the consistency score. As shown in Figure 3(c)-(d), in the beginning, the embeddings of classes are not well separated. However, during abductive learning, the distance between the different classes becomes larger after the neural net is updated with the abducted labels, which will in turn help accelerate the abduction.

Influence of Beam Width. We study the influence of beam width in optimization, and the results are presented in Table 2. The successful abduction increases as beam width becomes larger, while the time cost grows linear at the same time. The improvement becomes marginal when the beam width is larger than 1k. We use a beam width of 600 in our implementation to achieve the balance between convergence rate and time complexity.

6.4 Theft Judicial Sentencing

Table 3: Micro-F1-score of the model, and MAE of the predicted sentence. The label rates are denoted as suffixes.

KB	Method	F1	MAE
N/A	PL-10	0.814	0.862
N/A	Tri-10	0.812	0.840
Full	SS-ABL-10	0.862	0.824
Full	ABLSim-10	0.861	0.825
Part	SS-ABL-10	0.833	0.835
Part	ABLSim-10	0.851	0.828
N/A	PL-50	0.858	0.832
N/A	Tri-50	0.861	0.810
Full	SS-ABL-50	0.865	0.788
Full	ABLSim-50	0.866	0.786
Part	SS-ABL-50	0.862	0.803
Part	ABLSim-50	0.866	0.783

This is a real-world task in [13], which aims to train a model that outputs sentencing elements from criminal judgment texts, and optimize the parameters in knowledge base to predict the sentence of a defendant. We use the same knowledge base and BERT model [7] as in [13], where the knowledge base contains many law articles represented by logic rules. We additionally make the task more challenging by removing some pre-defined rules to weaken the background knowledge base [13].

We compare ABLSim with SS-ABL [13] and two semi-supervised methods Pseudo-Label (PL) [18] and Tri-training (Tri) [30]. It takes about 1 hour to train the model. As shown in table 3, ABL-based models are superior to the semi-supervised methods. When the number of labeled pre-train data is small (10%), the performance of ABLSim with weaker KB is even comparable to the SS-ABL with a full KB. When the number of labeled pre-train data increased to 50%, ABLSim achieves the highest performance with less pre-defined domain knowledge.

7 Conclusion

In this paper, we propose a novel consistency measure for abduction-based neuro-symbolic learning, and further present the Abductive Learning with Similarity (ABLSim) method. Compared to previous approaches, it not only exploits the full-featured logical reasoning ability, but also utilizes the information hidden in the feature space of the input data. The proposed consistency measure leverages the similarity between samples, which previous approaches have never considered. Empirical evaluation validates that ABLSim significantly outperforms the state-of-the-art neuro-symbolic learning approaches in terms of speed and performance with less labeled data. The proposed consistency measure is general, and any other abduction-based approach can use it. The limitation of the method is that the rules of the domain knowledge base need to be constructed manually. In future work, we will try to incorporate techniques like predicate invention into our approach to discover new classes and new knowledge, so that we can automatically extend the knowledge base.

Acknowledgments and Disclosure of Funding

This work is supported by the National Key Research and Development Program of China No.2020AAA0109400. Wang-Zhou Dai acknowledges the financial support from the UK’s EPSRC Robot Synthetic Biologist Project (EP/R034915/1). Stephen H. Muggleton wants to thank the support from EPSRC Network on Human-Like Computing (EP/R022291/1).

References

- [1] Yoshua Bengio. The consciousness prior. *arXiv preprint arXiv:1709.08568*, 2017.
- [2] Le-Wen Cai, Wang-Zhou Dai, Yu-Xuan Huang, Yu-Feng Li, Stephen Muggleton, and Yuan Jiang. Abductive learning with ground knowledge base. In *Proceedings of the 30th International Joint Conference on Artificial Intelligence (IJCAI)*, pages 1815–1821, 2021.
- [3] Ting Chen, Simon Kornblith, Mohammad Norouzi, and Geoffrey Hinton. A simple framework for contrastive learning of visual representations. In *Proceedings of the 37th International Conference on Machine Learning (ICML)*, pages 1597–1607, 2020.
- [4] Wang-Zhou Dai and Stephen H. Muggleton. Abductive knowledge induction from raw data. In *Proceedings of the 30th International Joint Conference on Artificial Intelligence (IJCAI)*, pages 1845–1851, 2021.
- [5] Wang-Zhou Dai, Qiuling Xu, Yang Yu, and Zhi-Hua Zhou. Bridging machine learning and logical reasoning by abductive learning. In *Advances in Neural Information Processing Systems 32 (NeurIPS)*, pages 2811–2822. 2019.
- [6] Luc De Raedt and Angelika Kimmig. Probabilistic (logic) programming concepts. *Machine Learning*, 100(1):5–47, 2015.
- [7] Jacob Devlin, Ming-Wei Chang, Kenton Lee, and Kristina Toutanova. Bert: Pre-training of deep bidirectional transformers for language understanding. *arXiv preprint arXiv:1810.04805*, 2018.
- [8] A Garcez, M Gori, LC Lamb, L Serafini, M Spranger, and SN Tran. Neural-symbolic computing: An effective methodology for principled integration of machine learning and reasoning. *Journal of Applied Logics*, 6(4):611–632, 2019.
- [9] Rebecca L Gómez and LouAnn Gerken. Infant artificial language learning and language acquisition. *Trends in cognitive sciences*, 4(5):178–186, 2000.
- [10] Alex Graves, Greg Wayne, Malcolm Reynolds, et al. Hybrid computing using a neural network with dynamic external memory. *Nature*, 538(7626):471–476, 2016.
- [11] Aditya Grover, Eric Wang, Aaron Zweig, and Stefano Ermon. Stochastic optimization of sorting networks via continuous relaxations. In *Sixth International Conference on Learning Representations (ICLR)*, 2018.
- [12] Kaiming He, Xiangyu Zhang, Shaoqing Ren, and Jian Sun. Deep residual learning for image recognition. In *Proceedings of the IEEE Conference on Computer Vision and Pattern Recognition (CVPR)*, pages 770–778, 2016.

- [13] Yu-Xuan Huang, Wang-Zhou Dai, Jian Yang, Le-Wen Cai, Shaofen Cheng, Ruizhang Huang, Yu-Feng Li, and Zhi-Hua Zhou. Semi-supervised abductive learning and its application to theft judicial sentencing. In *Proceedings of the 20th IEEE International Conference on Data Mining (ICDM)*, pages 1070–1075. IEEE, 2020.
- [14] John R Josephson and Susan G Josephson. *Abductive inference: Computation, philosophy, technology*. Cambridge University Press, 1996.
- [15] Daphne Koller, Nir Friedman, Sašo Džeroski, Charles Sutton, Andrew McCallum, Avi Pfeffer, Pieter Abbeel, Ming-Fai Wong, David Heckerman, Chris Meek, et al. *Introduction to statistical relational learning*. The MIT Press, 2007.
- [16] Alex Krizhevsky and Geoffrey Hinton. Learning multiple layers of features from tiny images. Technical report, University of Toronto, 2009.
- [17] Yann LeCun, Léon Bottou, Yoshua Bengio, and Patrick Haffner. Gradient-based learning applied to document recognition. *Proceedings of the IEEE*, 86(11):2278–2324, 1998.
- [18] Dong-Hyun Lee. Pseudo-label: The simple and efficient semi-supervised learning method for deep neural networks. In *ICML Workshop on Challenges in Representation Learning*, 2013.
- [19] Qing Li, Siyuan Huang, Yining Hong, Yixin Chen, Ying Nian Wu, and Song-Chun Zhu. Closed loop neural-symbolic learning via integrating neural perception, grammar parsing, and symbolic reasoning. In *Proceedings of the 37th International Conference on Machine Learning (ICML)*, pages 5884–5894. PMLR, 2020.
- [20] Lorenzo Magnani. *Abductive cognition: The epistemological and eco-cognitive dimensions of hypothetical reasoning*, volume 3. Springer Science & Business Media, 2009.
- [21] Robin Manhaeve, Sebastijan Dumancic, Angelika Kimmig, Thomas Demeester, and Luc De Raedt. Deepprolog: Neural probabilistic logic programming. In *Advances in Neural Information Processing Systems 31 (NeurIPS)*, pages 3749–3759. 2018.
- [22] Luc De Raedt, Sebastijan Dumancic, Robin Manhaeve, and Giuseppe Marra. From statistical relational to neuro-symbolic artificial intelligence. In *Proceedings of the 29th International Joint Conference on Artificial Intelligence (IJCAI)*, pages 4943–4950, 2020.
- [23] Luc De Raedt, Kristian Kersting, Sriraam Natarajan, and David Poole. Statistical relational artificial intelligence: Logic, probability, and computation. *Synthesis Lectures on Artificial Intelligence and Machine Learning*, 10(2):1–189, 2016.
- [24] Adam Santoro, David Raposo, David G Barrett, Mateusz Malinowski, Razvan Pascanu, Peter Battaglia, and Timothy Lillicrap. A simple neural network module for relational reasoning. In *Advances in Neural Information Processing Systems 30 (NIPS)*, pages 4967–4976. 2017.
- [25] Andrew Trask, Felix Hill, Scott E Reed, Jack Rae, Chris Dyer, and Phil Blunsom. Neural arithmetic logic units. In *Advances in Neural Information Processing Systems 31 (NeurIPS)*, pages 8035–8044. 2018.
- [26] Laurens Van der Maaten and Geoffrey Hinton. Visualizing data using t-sne. *Journal of Machine Learning Research*, 9(11), 2008.
- [27] Po-Wei Wang, Priya Donti, Bryan Wilder, and Zico Kolter. Satnet: Bridging deep learning and logical reasoning using a differentiable satisfiability solver. In *Proceedings of the 36th International Conference on Machine Learning (ICML)*, pages 6545–6554, 2019.
- [28] Zhi-Hua Zhou. A brief introduction to weakly supervised learning. *National science review*, 5(1):44–53, 2018.
- [29] Zhi-Hua Zhou. Abductive learning: towards bridging machine learning and logical reasoning. *Science China Information Sciences*, 62(7):76101, 2019.
- [30] Zhi-Hua Zhou and Ming Li. Tri-training: Exploiting unlabeled data using three classifiers. *IEEE Transactions on Knowledge and Data Engineering*, 17(11):1529–1541, 2005.